

REPORT DOCUMENTATION PAGE			Form Approved OMB NO. 0704-0188		
<p>The public reporting burden for this collection of information is estimated to average 1 hour per response, including the time for reviewing instructions, searching existing data sources, gathering and maintaining the data needed, and completing and reviewing the collection of information. Send comments regarding this burden estimate or any other aspect of this collection of information, including suggestions for reducing this burden, to Washington Headquarters Services, Directorate for Information Operations and Reports, 1215 Jefferson Davis Highway, Suite 1204, Arlington VA, 22202-4302. Respondents should be aware that notwithstanding any other provision of law, no person shall be subject to any penalty for failing to comply with a collection of information if it does not display a currently valid OMB control number.</p> <p>PLEASE DO NOT RETURN YOUR FORM TO THE ABOVE ADDRESS.</p>					
1. REPORT DATE (DD-MM-YYYY) 09-11-2016		2. REPORT TYPE Final Report		3. DATES COVERED (From - To) 18-Aug-2015 - 17-Aug-2016	
4. TITLE AND SUBTITLE Final Report: High Performance Computing and Visualization Infrastructure for Simultaneous Parallel Computing and Parallel Visualization Research			5a. CONTRACT NUMBER W911NF-15-1-0377		
			5b. GRANT NUMBER		
			5c. PROGRAM ELEMENT NUMBER 611103		
6. AUTHORS Suzanne Shontz, Weizhang Huang, Brian Laird, James Miller, Alessandro Salandrino, Daniel Voss, ZJ Wang, Zhongquan Charlie Zheng			5d. PROJECT NUMBER		
			5e. TASK NUMBER		
			5f. WORK UNIT NUMBER		
7. PERFORMING ORGANIZATION NAMES AND ADDRESSES University of Kansas 2385 Irving Hill Road Lawrence, KS 66044 -7568			8. PERFORMING ORGANIZATION REPORT NUMBER		
9. SPONSORING/MONITORING AGENCY NAME(S) AND ADDRESS (ES) U.S. Army Research Office P.O. Box 12211 Research Triangle Park, NC 27709-2211			10. SPONSOR/MONITOR'S ACRONYM(S) ARO		
			11. SPONSOR/MONITOR'S REPORT NUMBER(S) 66816-MA-RIP.11		
12. DISTRIBUTION AVAILABILITY STATEMENT Approved for Public Release; Distribution Unlimited					
13. SUPPLEMENTARY NOTES The views, opinions and/or findings contained in this report are those of the author(s) and should not be construed as an official Department of the Army position, policy or decision, unless so designated by other documentation.					
14. ABSTRACT The objective of this DURIP project was to acquire an HPC cluster and Mini CAVE to support research involving simultaneous parallel computing and parallel visualization at the University of Kansas (KU). We acquired HPC and visualization infrastructure that form a system for simultaneous parallel computing and parallel visualization research. The HPC cluster is composed of 17 compute nodes with 340 cores, 20 NVIDIA GPGPU's, and 14 Intel Co-Phi processors. The visualization infrastructure is a next generation tiled Mini CAVE for semi-immersive visualization. Our infrastructure leverages and extends existing KU infrastructure available to researchers through					
15. SUBJECT TERMS high performance computing, numerical analysis, scientific computing, scientific visualization, computational fluid dynamics, computational chemistry, computational electrodynamics					
16. SECURITY CLASSIFICATION OF:			17. LIMITATION OF ABSTRACT UU	15. NUMBER OF PAGES	19a. NAME OF RESPONSIBLE PERSON Suzanne Shontz
a. REPORT UU	b. ABSTRACT UU	c. THIS PAGE UU			19b. TELEPHONE NUMBER 785-864-8816

Report Title

Final Report: High Performance Computing and Visualization Infrastructure for Simultaneous Parallel Computing and Parallel Visualization Research

ABSTRACT

The objective of this DURIP project was to acquire an HPC cluster and Mini CAVE to support research involving simultaneous parallel computing and parallel visualization at the University of Kansas (KU). We acquired HPC and visualization infrastructure that form a system for simultaneous parallel computing and parallel visualization research. The HPC cluster is composed of 17 compute nodes with 340 cores, 20 NVIDIA GPGPU's, and 14 Intel Co-Phi processors. The visualization infrastructure is a next generation tiled Mini CAVE for semi-immersive visualization. Our infrastructure leverages and extends existing KU infrastructure available to researchers through the KU Advanced Computing Facility. The HPC and visualization system has supported research in five Department of Defense (DoD) mission-critical thematic areas involving simultaneous parallel computing and parallel visualization: unstructured meshing, scientific visualization, computational fluid dynamics, elastodynamics, and materials chemistry. The infrastructure has enhanced the research supported by and of interest to the DoD. It has enabled research projects involving: serial and parallel adaptive and moving mesh simulations, scientific visualizations, large eddy simulations of turbulent flows in gas engines, long-range acoustic propagation simulations, numerical modeling of nonlinear nanophotonic devices, and molecular dynamics simulations of solidification.

Enter List of papers submitted or published that acknowledge ARO support from the start of the project to the date of this printing. List the papers, including journal references, in the following categories:

(a) Papers published in peer-reviewed journals (N/A for none)

<u>Received</u>	<u>Paper</u>
-----------------	--------------

TOTAL:

Number of Papers published in peer-reviewed journals:

(b) Papers published in non-peer-reviewed journals (N/A for none)

<u>Received</u>	<u>Paper</u>
-----------------	--------------

TOTAL:

Number of Papers published in non peer-reviewed journals:

- (c) Presentations
1. 8th International Conference on Multi-scale Materials Modeling (MMM), Dijon, France, October 9-14, 2016 (Brian Laird, invited talk)
2. Physics Colloquium, University of Tübingen, Tübingen, Germany, October 16, 2016 (Brian Laird, invited talk)
3. Materials Science Colloquium, Rheinisch-Westfälische Technische Hochschule (RWTH), Aachen, Germany, November 9, 2016 (Brian Laird, invited talk).
- Number of Presentations: 3.00

Non Peer-Reviewed Conference Proceeding publications (other than abstracts):

Received	Paper
11/06/2016	5.00 . Future directions of high-fidelity CFD for aero-thermal turbomachinery research, analysis, and design, 46th AIAA Fluid Dynamics Conference. 05-JUN-16, Washington, D.C.. : ,
11/06/2016	6.00 . Recent progresses in large eddy simulations with the FR/CPR method, Ninth International Conference on Computational Fluid Dynamics (ICCFD9). 11-JUL-16, Istanbul, Turkey. : ,
TOTAL:	2

Number of Non Peer-Reviewed Conference Proceeding publications (other than abstracts):

Peer-Reviewed Conference Proceeding publications (other than abstracts):

Received	Paper
TOTAL:	

Number of Peer-Reviewed Conference Proceeding publications (other than abstracts):

(d) Manuscripts	
<u>Received</u>	<u>Paper</u>
TOTAL:	

Number of Manuscripts:

Books	
<u>Received</u>	<u>Book</u>
TOTAL:	

Received Book Chapter

TOTAL:

Patents Submitted

N/A

Patents Awarded

N/A

Awards

AIAA Fellow (ZJ Wang, 2015); University of Kansas Bellows Scholar Award (ZJ Wang, 2016), for outstanding accomplishments, including election as a Fellow of the American Institute of Aeronautics and Astronautics; AFOSR Young Investigator Award (Alessandro Salandrino, 2016); University of Kansas Miller Scholar Award for research excellence, including selection for the Air Force Office of Scientific Research Young Investigator Program (Alessandro Salandrino, 2016); University of Kansas Miller Scholar Award for research excellence including a DURIP award for high-performance computing and visualization instrumentation (Suzanne Shontz, 2016)

Graduate Students

<u>NAME</u>	<u>PERCENT SUPPORTED</u>	Discipline
Feilin Jia	0.00	
Cuong Ngo	0.00	
Yanan Li	0.00	
Susobhan Das	0.00	
Junjian Zhang	0.00	
Anpeng He	0.00	
FTE Equivalent:	0.00	
Total Number:	6	

Names of Post Doctorates

<u>NAME</u>	<u>PERCENT SUPPORTED</u>
Maurin Lopez Varilla	0.00
J. Pablo Palafox-Hernandez	0.00
FTE Equivalent:	0.00
Total Number:	2

Names of Faculty Supported

<u>NAME</u>	<u>PERCENT SUPPORTED</u>	National Academy Member
Suzanne Shontz	0.00	
Weizhang Huang	0.00	
Brian Laird	0.00	
James Miller	0.00	
Alessandro Salandrino	0.00	
ZJ Wang	0.00	
Zhongquan Charlie Zheng	0.00	
FTE Equivalent:	0.00	
Total Number:	7	

Names of Under Graduate students supported

<u>NAME</u>	<u>PERCENT SUPPORTED</u>
FTE Equivalent:	
Total Number:	

Student Metrics

This section only applies to graduating undergraduates supported by this agreement in this reporting period

The number of undergraduates funded by this agreement who graduated during this period: 0.00

The number of undergraduates funded by this agreement who graduated during this period with a degree in science, mathematics, engineering, or technology fields:..... 0.00

The number of undergraduates funded by your agreement who graduated during this period and will continue to pursue a graduate or Ph.D. degree in science, mathematics, engineering, or technology fields:..... 0.00

Number of graduating undergraduates who achieved a 3.5 GPA to 4.0 (4.0 max scale):..... 0.00

Number of graduating undergraduates funded by a DoD funded Center of Excellence grant for Education, Research and Engineering:..... 0.00

The number of undergraduates funded by your agreement who graduated during this period and intend to work for the Department of Defense 0.00

The number of undergraduates funded by your agreement who graduated during this period and will receive scholarships or fellowships for further studies in science, mathematics, engineering or technology fields: 0.00

Names of Personnel receiving masters degrees

NAME

Total Number:

Names of personnel receiving PHDs

NAME

Yanan Li

Total Number:

1

Names of other research staff

NAME

PERCENT SUPPORTED

Daniel Voss

0.00

FTE Equivalent:

0.00

Total Number:

1

Sub Contractors (DD882)

Inventions (DD882)

Scientific Progress

See Attachment

Technology Transfer

N/A

Scientific Progress and Accomplishments:

Foreword:

The objective of this DURIP project was to acquire an HPC cluster and Mini CAVE to support research projects involving simultaneous parallel computing and parallel visualization at the University of Kansas (KU). We acquired HPC and visualization infrastructure that together form a single system for simultaneous parallel computing and parallel visualization research. The HPC cluster is composed of 17 compute nodes with a total of 340 cores, 20 NVIDIA GPGPU's, and 14 Intel Co-Phi processors. The visualization infrastructure is a next generation tiled Mini CAVE for semi-immersive visualization. Our infrastructure leverages and extends existing KU infrastructure that is available to the researchers through the KU Advanced Computing Facility. (Further details on the simultaneous parallel computing and parallel visualization infrastructure can be found in Appendix A.)

The HPC and visualization system has supported research in five Department of Defense (DoD) mission-critical thematic areas involving simultaneous parallel computing and parallel visualization: unstructured meshing, scientific visualization, computational fluid dynamics, elastodynamics, and materials chemistry. The infrastructure has enhanced the quality of research supported by and of interest to the DoD. It has enabled research projects involving: serial and parallel adaptive and moving mesh simulations, scientific visualizations, large eddy simulations of turbulent flows in gas engines, long-range acoustic propagation simulations, numerical modeling of nonlinear nanophotonic devices, and molecular dynamics simulations of solidification.

Table of Contents:

Page 1: Foreword

Page 2: Table of Contents

Page 3: List of Appendices, Illustrations, and Tables

Page 4: Scientific Progress and Accomplishments

Page 12: Appendix A: Equipment Purchased

Page 16: Appendix B: Special Circumstances in Acquisition of Infrastructure

List of Appendices, Illustrations, and Tables:

Appendices:

Page 12: Appendix A: Equipment Purchased

Page 16: Appendix B: Special Circumstances in Acquisition of Infrastructure

Illustrations:

Page 5: Figure 1: Average mesh quality versus number of iterations on an 80M element tetrahedral mesh

Page 5: Figure 2: (a) Total runtime and (b) speedup for the Parallel VMQI algorithm for the same 80M element tetrahedral mesh

Page 7: Figure 3: Pressure contours of ultrasound propagation at different moments: (a) $t=12\mu\text{s}$ (b) $t=20\mu\text{s}$ (c) $t=24\mu\text{s}$ (d) $t=30\mu\text{s}$

Page 8: Figure 4: Effects of moving source on sound pressure power-spectrum density for an airplane flying at 50 m/s with the source represented by a harmonic Gaussian source at the frequency of 300 Hz, with the receiver location the same altitude as the airplane flight path: (a) free space propagation; (b) a rigid ground

Page 8: Figure 5: ITO MOS nanophotonic modulator layout.

Tables:

N/A

Scientific Progress and Accomplishments

For each of the seven investigators on the team, we give a statement of the problem studied, a summary of the most important results, and a bibliography.

Investigator: Weizhang Huang

Statement of the problem studied: The porous medium equation models nonlinear diffusion processes that arise from several branches of science such as gas flow in porous medium, incompressible fluid dynamics, nonlinear heat transfer, and image processing. Its numerical simulation includes several challenges including dealing with diffusion degeneracy and moving free boundaries and necessary use of dynamical mesh adaptation for improving computational efficiency and accuracy. In this project, we have studied the numerical solution of the porous medium equation using an adaptive moving mesh finite element method. The method is based on the moving mesh partial differential equation approach and employs its newly developed implementation.

Summary of the most important results: The method shows a first-order convergence for uniform and arclength-based adaptive meshes and a second-order convergence for Hessian-based adaptive meshes. It is also shown that the method can be used for situations with complex free boundaries, emerging and splitting of free boundaries, and the porous medium equation with variable exponents and absorption. The results obtained so far are summarized in an article submitted to Journal of Computational Physics [1].

Bibliography:

[1] C. Ngo and W. Huang, A study on moving mesh finite element solution of the porous medium equation, Journal of Computational Physics (submitted, under revision)

Investigator: Suzanne Shontz

Statement of the problem studied: Parallel mesh quality improvement is needed whenever meshes of low quality arise in computationally-intensive simulations. An example of such problems is the direct numerical simulations for fluid-structure interactions. In particular, mesh quality improvement methods improve the efficiency and accuracy of the associated numerical PDE algorithm and also maintains its stability. There are very few parallel variational methods for mesh quality improvement. Therefore, we study effective parallelization strategies for a variational mesh quality improvement method proposed by Huang and Kamenski [2,3].

Summary of the most important results⁴: We have developed a parallel variational mesh quality improvement algorithm designed for distributed memory machines (Figure 1). The new parallel algorithm is based on the sequential variational mesh quality improvement method proposed by Huang and Kamenski [2,3]. To distribute the workload among processors, our parallel implementation employs a partition of the mesh, which is generated using METIS. The algorithm solves an ordinary differential equation on each interior node of each region created by the partition of the mesh. For the nodes that belong to the shared boundaries, only a partial ODE solution is calculated initially, as these nodes are shared among cores. The ODE solution at the shared nodes is completed by adding the partial solutions of each processor. This operation is performed using non-blocking MPI collective communication instructions to overlap communication with computation. We use tetrahedral meshes with different sizes to test the strong and weak scaling of our implementation. The numerical experiments, performed

using up to 128 processors, demonstrate the excellent strong scalability of our implementation when tested on meshes with 80M and 40M elements (Figure 2). The weak scaling results are typical of those obtained on unstructured meshes.

In the future, we plan to visualize our parallel adaptive, moving meshes in the Mini-CAVE environment which will help us in understanding the performance of our algorithms.

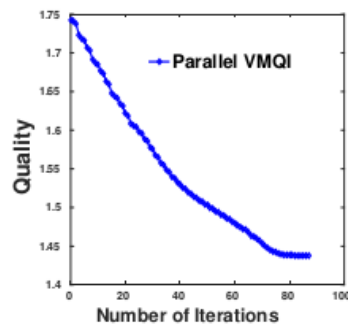


Fig. 1: Average mesh quality vs. number of iterations for an 80M element tetrahedral mesh.

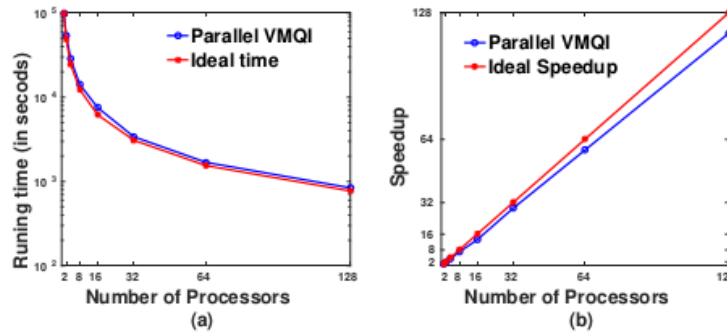


Fig. 2: (a) Total runtime and (b) speedup for the Parallel VMQI algorithm for the same 80M element tetrahedral mesh.

Bibliography:

- [2] W. Huang, L. Kamenski, H. Si, Mesh smoothing: an MMPDE approach. Research note at the 24th Int. Meshing Roundtable (2015).
- [3] W. Huang, L. Kamenski, A geometric discretization and a simple implementation for variational mesh generation and adaptation, J Comput Phys, Vol. 301, pp. 322-337, (2015).
- [4] M. Lopez, S.M. Shontz, and W. Huang, An efficient parallel implementation for a variational mesh quality improvement method, To be submitted to Engineering with Computers, November 2016.

Investigator: James Miller

Statement of the problem studied: The problem under investigation was the determination of the best way to support stereo rendering on the mini-CAVE display environment.

Summary of the most important results: A basic OpenGL graphics framework developed by Dr. Miller and used for both teaching and research projects was modified to support stereo rendering on the mini-CAVE display environment. A review of the literature was performed, which resulted in three variations for stereo view matrix generation. Two of these variations have been previously described in various papers. Two other variations will also be examined. In addition, several heuristics for establishing good stereo viewing parameters will be pursued. Some of these heuristics for obtaining good stereo viewing performance have been described in the literature, whereas others are independent ideas to be pursued. An evaluation will be performed in which it will be determined how the variations and heuristics compare to one another so that optimal ones can be quickly, and hopefully automatically, generated.

Bibliography: N/A

Investigator: ZJ Wang

Statement of the problem studied: We employed the infrastructure to perform large eddy simulations for turbulent flows in a gas turbine engine.

Summary of the most important results: The results are compared with experimental data, and very good agreement has been achieved. A movie is here: http://dept.ku.edu/~cfdku/LES_turbine_Q_sch.gif Two papers have been published summarizing: future directions of high-fidelity computational fluid dynamics for aero-thermal turbomachinery [5] and large eddy simulations results based on the FR/CPR method [6].

Bibliography:

[5] G.M. Laskowski, J. Kopriva, V. Michelassi, S. Shankaran, U. Paliath, R. Bhaskaran, Q. Wang, C. Talnikar, Z.J. Wang, F. Jia, Future Directions of High-Fidelity CFD for Aero-Thermal Turbomachinery Research, Analysis and Design, AIAA-2016-3322.

[6] Z.J. Wang and Y. Li, Recent Progresses in Large Eddy Simulations with the FR/CPR Method, Ninth International Conference on Computational Fluid Dynamics (ICCFD9), Istanbul, Turkey, July 11-15, 2016, ICCFD9-2016-149.

Investigator: Zhaoquan Charlie Zheng

Statement of the problem studied: Time-domain simulations of ultrasound propagation with fractional Laplacian were conducted. Similarly, physical simulations of sound propagation from aircraft to close proximity to the ground were performed.

Summary of the most important results: With the help of the computer facility purchased using the grants, the following DoD related computational research projects have been conducted:

Time-domain simulation of ultrasound propagation with fractional Laplacian: The simulation is developed for the purpose of simulating ultrasound propagation through biological tissues. The simulation is based on the time-domain conservation laws with the governing equations for acoustic pressure and velocity, with frequency dependent absorption and dispersion effects. We use forward differencing for velocity and backward differencing for pressure on the non-fractional derivative operator terms in spatial discretization. The fractional Laplacian operators are treated as Riesz derivatives. The shifted standard Grunwald approximation method is used to solve fractional derivative operator terms. To accommodate complicated biological tissue geometries, an immersed boundary method is developed that enables a Cartesian computational grid mesh to be used. The results are compared with those for a non-absorption homogeneous medium to discuss absorption and dispersion effects of biological material. Figure 3(a)-(d) are pressure contours at four different moments. Sound wave propagation and attenuation through the biological bone model can be clearly observed. Reflections can be observed when the ultrasonic plane waves enter the bone medium, due to the absorption and dispersion of the waves inside the bone. In Figure 3(d), it shows acoustic pressure of the plane wave dramatically attenuated by the lossy bone media comparing with the original waves in 3(a). Meanwhile there are several reflected waves remaining inside the bone. This research was partly supported by ARL under a cooperative agreement W911-NF-14-2-0077.

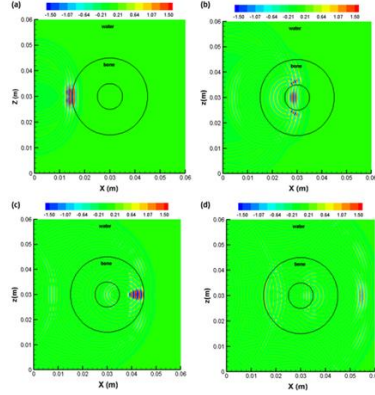


Fig. 3: Pressure contours of ultrasound propagation at different moments:
(a) $t=12\mu s$ (b) $t=20\mu s$ (c) $t=24\mu s$ (d) $t=30\mu s$.

Physical simulation of sound propagation from aircraft in close proximity to the ground: This study is to investigate sound propagation from aircraft to the environment. The sound propagation is simulated based on the physical time and space, which is a time-domain simulation in a physical spatial domain. The investigation will be focused on the physics that is usually difficult to reveal using frequency-domain simulations. The effects to be investigated include source characteristics and motion of aircraft, influence of local environment such as ground roughness and impedance, diffraction caused by local structures such as terrain, buildings, bushes and trees. Because the special interest of the study is for aircraft in close proximity to the ground, such as UAVs, these effects are more significant for sound propagation than for the cases when aircraft are at higher altitude from the ground. Examples of source recognition using the simulation results are discussed. Figure 4 shows the Doppler effects caused by the aircraft motion both in free-space propagation and with the rigid ground reflection. The motion of the airplane causes the harmonic frequency at 300 Hz to shift both higher and lower. The Doppler shifts are caused by the airplane flying towards and away from the receiver, with a theoretical estimate of $\left(1 \pm \frac{V}{c}\right)f$, where V is the airplane flying speed at 50 m/s, c is the speed of sound at 340 m/s, and f is the harmonic source frequency at 300 Hz. The plus shift is when the airplane is flying towards the receiver location and the minus is when the airplane is flying away from the receiver location. The resultant higher and lower frequencies based on this formula are respectively 344 Hz and 256 Hz. These frequency values are very close to the two peak frequencies for the moving source results shown in Fig. 4 for both free space, Fig. 4(a) and with a rigid ground, Fig. 4(b). This research was partly supported by ARL under a cooperative agreement W911-NF-14-2-0077.

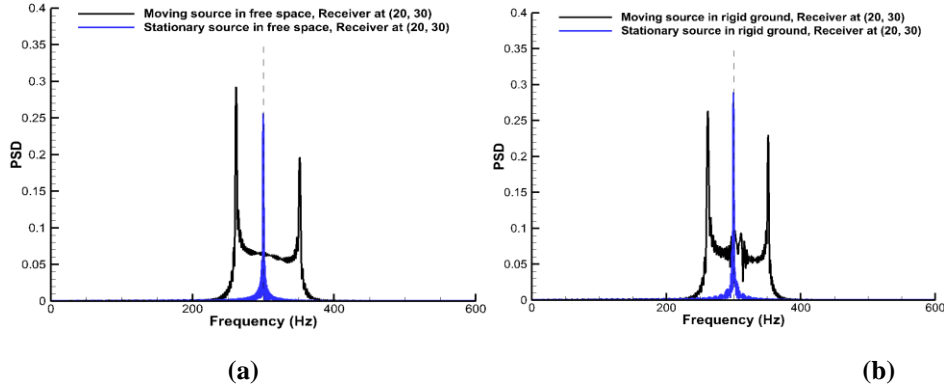


Fig. 4: Effects of moving source on sound pressure power-spectrum density for an airplane flying at 50 m/s with the source represented by a harmonic Gaussian source at the frequency of 300 Hz, with the receiver location the same altitude as the airplane flight path: (a) free space propagation; (b) a rigid ground.

Bibliography: N/A

Investigator: Alessandro Salandrino

Statement of the problem studied: Metamaterials are artificially engineered media which are structured at a deeply sub-wavelength length-scale to provide a macroscopic electromagnetic response with properties not found in natural materials. Examples include negative index metamaterials [7, 8], hyperbolic dispersion media [9] or epsilon/mu-near-zero materials [10]. The analysis and design of metamaterial-based devices is especially challenging from the computational point of view because of the length-scales involved: while the devices themselves have dimensions of the order of the relevant wavelength, the structures which provide the desired functionalities are much smaller and require an extremely fine discretization. The availability of the high performance computing facilities acquired under the US Army Research Office grant W911-NF-1510377 has proven essential in order to design and simulate novel nonlinear nanophotonic devices.

In this project so far we concentrated on the analysis and design of nanophotonic modulators with optical nonlinearities originating from voltage-gated free-carrier injection in Indium-Tin-Oxide (ITO) metal-oxide-semiconductor (MOS) structures (Fig. 5). Such devices require the concurrent modeling and optimization of the following characteristics (with the corresponding relevant length-scales:

1. Electronic properties of the materials (sub-nm length-scale)
2. Electrostatic properties of the MOS structure (sub- μm length-scale)

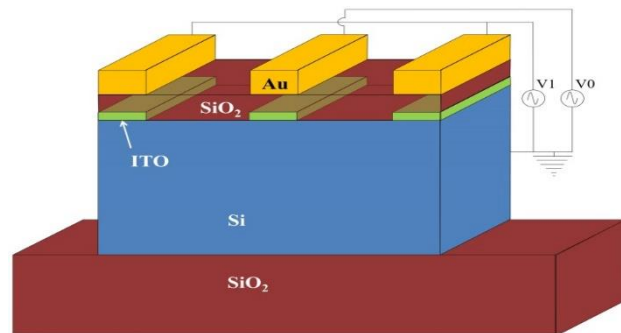


Fig. 5. ITO MOS nanophotonic modulator layout.

3. Electromagnetic and modal properties of the device in its entirety (μm length-scale)

The main modeling challenges arise in combining the electronic modeling with the other two aspects, due to the large difference in characteristic lengths. Moreover, any modification/optimization of the geometry requires a reevaluation of all of the three design components – electronic, electrostatic, and electromagnetic.

The main goal of this effort was to fully exploit the unique properties of ITO to design a photonic device with enhanced functionalities. ITO is a degenerately doped semiconductor with free-carrier concentration that can be tuned by controlling the concentration of oxygen vacancies and interstitial metal dopants. In addition to doping, carrier concentration can also be electrically tuned. Near-unity index changes by carrier injection in ITO have been recently reported [11, 12]. Such large refractive index changes occur within a charge-accumulation layer induced by an electrostatic bias at the interface between ITO and an insulating medium (in our case silicon dioxide). Modeling the electromagnetic behavior of the ITO in the accumulation layer poses challenges because a strong concentration gradient occurs within a sub-nanometer thickness – i.e. over a length-scale which is three orders of magnitude below the intended wavelength of operation ($\sim 1550\text{nm}$). If accurately modeled and understood, such free-carrier effects in ITO can be effectively exploited to design ultra-compact photonic electro-absorption modulators.

Summary of the most important results: In the span of one year since the beginning of this project under the US Army Research Office grant W911-NF-1510377 support we have successfully addressed most of the research tasks stated in the previous section, with the following main results:

1. We designed and optimized in all its aspects (electronic, electrostatic, and electromagnetic) an ITO-based nanophotonic modulator architecture.
2. Based on the results that we obtained we introduced the concept of modal-dichroism in nanophotonics, which paves the way towards a novel class of ultra-compact mode-multiplexed nanophotonic devices.
3. We have reported our results in the journal article [7] and we acknowledged US Army Research Office support.

The results obtained so far have opened a new research line in Dr. Salandrino's group, which will likely lead to additional novel device concepts in the months to come.

Bibliography:

- [7] J. B. Pendry, "Negative refraction makes a perfect lens," *Phys. Rev. Lett.* **85**, 3966-3969 (2000).
- [8] A. Alu, A. Salandrino, and N. Engheta, "Negative effective permeability and left-handed materials at optical frequencies," *Opt Express* **14**, 1557-1567 (2006).
- [9] A. Salandrino, and N. Engheta, "Far-field subdiffraction optical microscopy using metamaterial crystals: Theory and simulations," *Phys. Rev. B* **74**, 5 (2006).
- [10] A. Alù, M. G. Silveirinha, A. Salandrino, and N. Engheta, "Epsilon-near-zero metamaterials and electromagnetic sources: Tailoring the radiation phase pattern," *Phys. Rev. B* **75**, 155410 (2007).
- [11] E. Feigenbaum, K. Diest, and H. A. Atwater, "Unity-order index change in transparent conducting oxides at visible frequencies," *Nano Lett.* **10**, 2111-2116 (2010).
- [12] V. J. Sorger, N. D. Lanzillotti-Kimura, R.-M. Ma, and X. Zhang, "Ultra-compact silicon nanophotonic modulator with broadband response," *Nanophotonics* **1**, 17-22 (2012).

[13] S. Das, S. Fardad, I. Kim, J. Rho, R. Hui, and A. Salandrino, "Nanophotonic modal dichroism: mode-multiplexed modulators," *Opt. Lett.* **41**, 4394-4397 (2016).

Investigator: Brian Laird

Statement of the problem studied: Most solidification occurs via heterogeneous nucleation, but atomistic studies of this technologically important phenomenon are rare. Using the GPU resources provided by the DURIP grant, we have examined the effect of interfacial structure and orientation on the heterogeneous nucleation of Pb crystals from the supercooled melt at a Cu substrate using molecular-dynamics (MD) simulation, as implemented in the highly parallel simulation code LAMMPS. In a previous work studying the Cu/Pb solid-liquid interface with MD simulation [14], we observed that the structure of the Cu(111) and Cu(100) interfaces were significantly different at 625K, just above the Pb melting temperature (618K for the model). The Cu(100) interface exhibited significant surface alloying in the crystal plane in contact with the melt. In contrast, no surface alloying was seen at the Cu(111) interface; however, a prefreezing layer of crystalline Pb, 2-3 atomic planes thick and slightly compressed relative to bulk Pb crystal, was observed to form at the interface. Because of the large difference in interfacial structure between the (100) and (111) interfaces, this system provides an excellent test-bed to study the orientation and surface structure dependence of heterogeneous nucleation.

Summary of the most important results: ¹⁵We observe that the Cu(111) interface the prefreezing layer is no longer present at 750K, but surface alloying in the Cu(100) interface persists. In a series of undercooling MD simulations, heterogeneous nucleation of fcc Pb is observed at the Cu(111) interface within the simulation time (5 ns) at 592K - a 26K undercooling. Nucleation and growth at Cu(111) proceeded layer-wise with a nearly planar critical nucleus. Quantitative analysis yielded heterogeneous nucleation barriers that are more than two orders of magnitude smaller than the predicted homogeneous nucleation barriers from classical nucleation theory. Heterogeneous nucleation was considerably more difficult on the Cu(100) surface alloyed substrate. An undercooling of approximately 170K was necessary to observe nucleation at this interface within the simulation time. From qualitative observation, the critical nucleus showed a contact angle with the Cu(100) surface of over 90°, indicating poor wetting of the Cu(100) surface by the nucleating phase, which according to classical heterogeneous nucleation theory provides an explanation of the large undercooling necessary to nucleate on the Cu(100) surface, relative to Cu(111), whose surface is more similar to the nucleating phase due to the presence of the prefreezing layer. The GPU resources were instrumental in completing this work due to the computational intensity of collecting nucleation statistics.

Current and future work: We will continue to use the GPU resources provided by the DURIP grant to study other metal-metal and metal-insulator solid-liquid interfaces. Two specific systems currently under study are gallium-aluminum, which is an important test case to study the phenomenon of liquid-metal embrittlement, and alumina-aluminum, a system for which experimental data is available for the structure of the solid-liquid interface allowing for a rare comparison of simulation with experiment for solid-liquid interfaces. There is potential in these systems to also use the Phi-based CPUs provided in the grant, but currently the Phi version of LAMMPS is very limited, but should be available for the systems here in the near future. For the alumina-aluminum systems, the visualization capabilities made possible with the Mini-CAVE should also prove useful.

Bibliography:

- [14] J.P. Palafox-Hernandez, M.D. Asta and B.B. Laird, *Acta Mater.* **59**, 3137 (2011)
- [15] J.P. Palafox-Hernandez and B.B. Laird, *J. Chem. Phys.*, **145**, 211914 (2016)

Appendix A: Equipment Purchased

HPC Equipment:

Quantity (10) Standard Compute Unit (SCU) with (2) NVIDIA K80 GPGPUs \$148,935.70
Dell PowerEdge R730
Mellanox ConnectX-3, Single Port, VPI FDR, QSFP+ Adapter
Broadcom 5720 QP 1Gb Network Daughter Card
(2) Intel Xeon E5-2680 v3 2.5GHz, 30M Cache, 9.60GT/s QPI, Turbo, HT, 12C/24T (120W)
Max Mem 2133 MHz
128GB RDIMM, 2133 MT/s, Dual Rank, x4 Data Width
1TB 7.2K RPM SATA 6Gbps 3.5in Hot-plug Hard Drive
600GB Panasas network storage

Quantity (7) Standard Compute Unit (SCU) with (2) Intel Phi 7120p Accelerators \$89,104.75
Dell PowerEdge R730
Mellanox ConnectX-3, Single Port, VPI FDR, QSFP+ Adapter
Broadcom 5720 QP 1Gb Network Daughter Card
(2) Intel Xeon E5-2680 v3 2.5GHz, 30M Cache, 9.60GT/s QPI, Turbo, HT, 12C/24T (120W)
Max Mem 2133 MHz
128GB RDIMM, 2133 MT/s, Dual Rank, x4 Data Width
1TB 7.2K RPM SATA 6Gbps 3.5in Hot-plug Hard Drive
600GB Panasas network storage

Total: **\$238,040.45**

Visualization Equipment:

ITEM	QTY	COST/UNIT	EXTENDED
Mechdyne Next Generation Ultra-High-Definition Mini CAVE System	1	\$245,919	\$245,919
• <i>Next Generation Tiled Mini CAVE:</i> Six (6) passive stereo 46" displays, One (1) moveable cart with integrated equipment rack, travel cases.	1	Included	Included
• <i>Tracking System:</i> ART SMARTTRACK with Wand and Head Tracker markers. <u>Includes one spare wand w/ tracking target and one spare head tracking target.</u>	1	Included	Included
• <i>Laptop Wired Connection Point:</i> Extron Pro Scalar with Auto Aspect Ratio Control, VGA, DVI, HDMI, or DisplayPort Connection.	1	Included	Included
• <i>3D System:</i> Twelve (12) Pairs Passive 3D Glasses from the display manufacturer.	1	Included	Included
• <i>USB Switching and Extension:</i> One (1) Wireless Keyboard and Mouse; One (1) 1RU Rack-mounted Pull-Out 19" Monitor/Keyboard/Mouse Drawer.	1	Included	Included
• <i>Main Rendering Workstation:</i> Minimum Specifications Include: * 4 RU Tower * 2 CPU, Xeon, 8core/16thread, 3.2GHz (E5-2667v3) * 128GB RAM * SSD, 2.5", 512GB * HDD, 3.5", 4TB * ODD, BD/DVD/CD read/write * OS, Microsoft Windows 7 Professional x64 SP1 * Rack mounting rails * 4 GPU, NVIDIA Quadro M5000 (8GB) * 1 GSU, NVIDIA K-Series Quadro Sync Kit	1	Included	Included
• <i>Cabling Lot, Adaptors, Terminations, and Consumables</i>	1	Included	Included
• <i>Mechdyne Design and Integration:</i> AV Design, Mechanical Design, Applications Engineering, Project Management, Staging, & Installation	1	Included	Included
• <i>Mechdyne Travel and Living Total:</i>	1	Included	Included
• <i>Mechdyne Shipping and Handling:</i>	1	Included	Included

Mechdyne Software

<ul style="list-style-type: none"> • Conduit configured for the Mini-CAVE system <ul style="list-style-type: none"> • Supports 3D passive stereo viewing and user perspective with the tracking system. • Conduit for Visit, TecPlot, TetGen/TetView, Google Earth, Sketchup • Includes one (1) year of remote support and upgrades 	1	Included	Included
<ul style="list-style-type: none"> • getReal3D for Unity configured for the Mini-CAVE system <ul style="list-style-type: none"> • Supports 3D passive stereo viewing and user perspective with the tracking system. • Includes one (1) year of remote support and upgrades • Requires Unity Pro for development (not included) 	1	Included	Included
<ul style="list-style-type: none"> • On-site software usage training included (one day for initial Development System and one day for mini-CAVE system) 	1	Included	Included

Maintenance Support

<ul style="list-style-type: none"> • Pricing for year 1 	1	\$7,080	\$7,080
		1 year Total	\$7,080

- *1 System Support visits*- System Support visits are one day visits used to provide quick unscheduled response to resolve system issues and provide onsite parts replacement. System Support onsite response time of 72 hours.
- *Mechdyne parts coverage*- Parts coverage provides warranty for all components of your system. Consumables are excluded but a quote for consumable coverage can be provided.
- *24/7 unlimited telephone and email support*- Phone and email support will help resolve minor issues immediately
- *Access to PIVOT*- PIVOT allows clients to log into our service database and create repair tickets for their system issues. You then have access to track the status of your repair and see the final report when the repair is complete.
- *Priority repair service* - Priority service is provided to our contract clients. This means you will be serviced before those who do not have contracts.
- *Discounted labor rates* - Maintenance contract clients receive discounted labor rates for any work provided that is not covered under the maintenance contract.
- Other exclusions, limitations, terms, and conditions may apply to the Mechdyne Service and Warranty solutions. Please speak with your account representative for a comprehensive support proposal.

Development System

- | | | | |
|--|---|----------|----------|
| • <i>3D Display with Mounting Cart:</i> One (1) 60" UHD Resolution (3840x2160) passive stereo display, One (1) display mount cart with castors. Includes 10 pairs of stereo glasses from the display manufacturer. | 1 | Included | Included |
| • <i>Spare Panels:</i> One (1) 60" UHD Resolution (3840x2160) passive stereo display, | 1 | Included | Included |

Note: The display proposed here is a consumer-grade television display. It will likely only have a 90 day warranty in a commercial application. This is not a professional grade panel, is not rated for continuous use, and we cannot guarantee availability of replacements, parts, or related beyond one year due to rapid model changes of consumer grade flat panel displays. As a result, we are providing this one spare panel.

Total	<hr/>	\$252,999
-------	-------	-----------

Appendix B: Special Circumstances in Acquisition of Infrastructure

The Mechdyne original proposed configuration of the Mini-cave encountered a delay because the company that manufactures the 46" display panels, Planar, shut down their manufacturing plant shortly after the grant period to upgrade their production line to produce higher resolution panels (from 720p to 1080p). The original 720p panels that were quoted for the Mini-cave system were unavailable due to large orders from customers already in process. We were one of the first customers in line to purchase the new 1080p panels when manufacturing resumed. The panels are specialized, non-consumer grade displays that cannot be replaced by standard panels.

To compensate KU for the delay, a temporary, replacement Mini-cave configuration was provided from Mechdyne in March, 2016, for no additional charge, with a matrix of 1 x 3 consumer grade 60" 4K 3-D displays (the original configuration was a 2 x 3 matrix of 46" 3-D displays). This provided a comparable platform for researchers to use for the visualization simulations. When manufacturing resumed and the Planar panels were available in June, 2016, Mechdyne built and tested the Mini-cave and delivered it to KU the second week of July, 2016.

A second delay for some of the researchers who use a Linux environment for their visualizations was due to a mixup between the Mechdyne sales team and the quoted configuration for the Mini-cave. KU was led to believe there would be support for a dual-boot operating system (Windows and Linux) and the Mechdyne visualization software environment. After some discussions about the mixup, it was decided KU would install and support the Linux operating system and Mechdyne would install and test their visualization software environment, but with only software support for the Windows versions of the software. The configuration of the Linux environment by Mechdyne encountered additional delays due to compatibility with NVIDIA drivers for the multi-display and multi-GPU configuration.